

Performance Comparison of PI and IP Controllers Used to Control a DC Machine Powered by a Photovoltaic Generator

Abdelhak Bouchakour^{#1}, Abdelhalim Borni^{#2}, Layachi Zaghba^{#3}, Mostéfa Brahami^{*4}, Hadj Mahammed Idriss^{#5}

[#] Unité de Recherche Appliquée en Energies Renouvelables, URAER,

Centre de Développement Des Energies Renouvelables, CDER, 47133 Ghardaïa, Algeria

¹abdelhak.bouchakour@yahoo.fr

²borni.abdelhalim@yahoo.fr

³layachi40@yahoo.fr

⁵hmidriss65@yahoo.fr

^{*}Intelligent Control and Electrical Power Systems
Université Djillali Liabès de Sidi Bel Abbès, Algérie

Département de l'électrotechnique

²mbrahami@yahoo.com

Abstract— In this article, we will make a comparison between the performances of two conventional control techniques for controlled speed and expected courant. The purpose is to evaluate the method that gives the best dynamic response (speed without going beyond) between the regulator classic PI type and IP. The comparison between the two methods under the same conditions is illustrated through simulations.

Keywords— the photovoltaic energy, PI and IP controller; photo current; DC/DC inverter.

I. INTRODUCTION

The photovoltaic (PV) energy conversion is now recognized to be most widely accepted method of harnessing renewable energy sources to benefit communities, especially in developing countries and remote areas. PV arrays provide direct conversion of solar energy into electrical energy, which is by far the most, sought after form of energy for human activities. Recognizing these fact extensive research and development efforts devoted to photovoltaic. One of the most popular applications of the PV array utilization is the water pumping system using DC motors as drive [1][2].

However to utilize PV power more efficiently a mean of load matching between PV array and DC motor as an intermediate matching circuitry is essential. Utilization of buck boost converters has been considered for this purpose and successful results have been recorded. However investigations are devoted steady-state operations. Dynamics have not considered which is important for system sizing and safe operation. This present study, therefore devoted to the dynamics of the PV array-boost converter powered DC motor driving a pump. Complete system is modeled in time domain and necessary computer algorithm is developed.

In this work, the dynamic performance of a system which uses is studied, to optimize system performance data, the system must be controlled by using two types of current and speed regulators: the classical (PI) and (IP).[3][7]

II. IDENTIFICATION OF THE PV SYSTEM

The system is composed of a PV generator, an MPPT power adapter, a DC/DC inverter, and a submerged pump.

A. Electrical Model for a Photovoltaic Cell

The PV cell is simulated by the single-diode model; the general formula of the PV characteristic is represented in figure 1 [2][4][5]

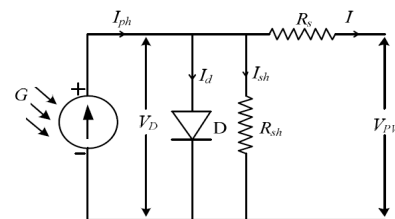


Fig.1. the Simulink PV-cell model scheme

$$I = I_{ph} - I_d - I_{sh}$$

$$I_{ph} = I_{sc} \left(\frac{\varphi}{1000} \right),$$

$$I_{sc} = I_{scref} [1 + k_0 (T - T_{ref})],$$

$$I_d = I_0 \left(e^{\frac{q(V+R_s I)}{nkT}} - 1 \right),$$

$$I_0 = I_{0(Tref)} \left(\frac{T}{T_{ref}} \right)^{\frac{3}{n}} \exp \left[\frac{-qE_g}{nk} \left(\frac{1}{T} - \frac{1}{T_{ref}} \right) \right],$$

$$I_r = \frac{V + R_s I}{R_{sh}},$$

$$I = I_{sc} \left(\frac{\phi}{1000} \right) - I_0 \left(e^{(V+R_s I)/V_T} \right) - \frac{V+R_s I}{R_{sh}}$$

Where:

- I_{ph} The photo current proportional to the solar radiation cell ϕ
- I_{sc} The short-circuit current.
- I_0 The current through the diode
- T The temperature cell
- k_0 Temperature sensitivity
- q Electron charge ($1.6 \cdot 10^{-19} [C]$)
- k Boltzmann constant ($1.38 \cdot 10^{-23} [j/k]$)
- n Ideality of the solar cell factor between 1 and 5 in practice.

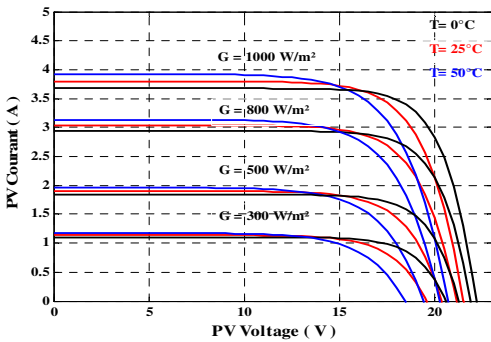


Fig.2 Characteristic I (V) at T=25°C

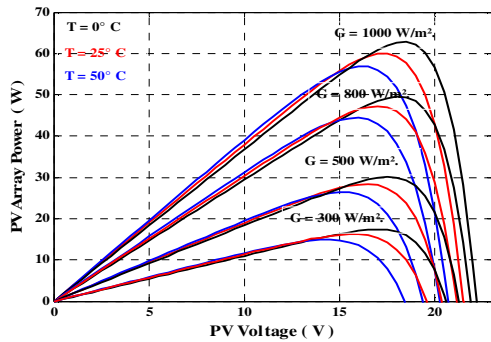


Fig.3 Characteristic P (V) at G=1000W/m2

B. The Buck-Boost Convert

This converter has the capability of scaling and of amplifying the constant input voltage source value V_{pv} at the output. The fundamental difference in our converter is that this new converter does not change the polarity of the input voltage source V_{pv} at the output.

The dynamic model of the solar subsystem written in terms of voltage and current between the input and the output of the buck-boost converter can be expressed as follows:

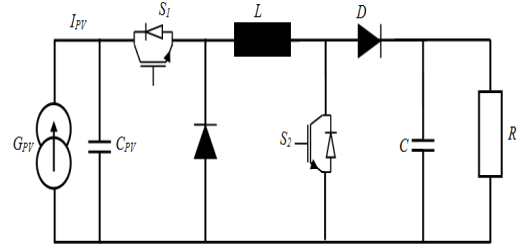


Fig.4 Simplified diagram of a non-reversible Buck-Boost Converter

$$\begin{cases} \frac{dV_{PV}}{dt} = \frac{i_{PV}}{C_{PV}} - \frac{i}{C_{PV}} u \\ L \frac{di}{dt} = (1-u)V + uV_{PV} \\ C \frac{dV}{dt} = -(1-u)i - \frac{V}{R} \end{cases}$$

Where I_{pv} is the injected current into the DC-DC converter. L , C are the electrical parameters DC-DC converter, u is the use coefficient.

C. Modeling of a Permanent Magnet DC Motor

The mathematical relation that describes the dynamic model of a DC motor with constant magnetic flux can be expressed as follows: [1][6]

$$e_a = i_a R_a + L_a \frac{di_a}{dt} + e$$

Where e_a is the applied voltage, e is the motor e.m.f. The e.m.f. of a permanent magnet motor can be expressed as:

$$e = K_E \omega_m$$

The electromagnetic torque is related to the armature current by:

$$T_e = K_T i_a$$

K_E The back e.m.f constant

K_T The torque constant

L_a The armature induction [H]

R_a The armature resistance [Ohm]

i_a The armature current [A]

ω_m The rotor angular speed [rad/s]

D. Model of the Centrifugal Pump

The HQ characteristic of the centrifugal pump is shown below. The expression of the total nanometric head is given by the model of Pleider-Peterman [7][8]

$$H = C_1 \cdot \omega_m^2 + C_2 \cdot Q \cdot \omega_m - C_3 \cdot Q^2$$

C_1 , C_2 and C_3 : are constants given by the manufacturer.

The mechanical and hydraulic powers are given by:

$$P_H = \rho \cdot g \cdot Q \cdot H$$

$$P_{mec} = K_P \cdot \omega_m^3$$

Q: flow rate of water (m3/sec).
H: nanometric high.

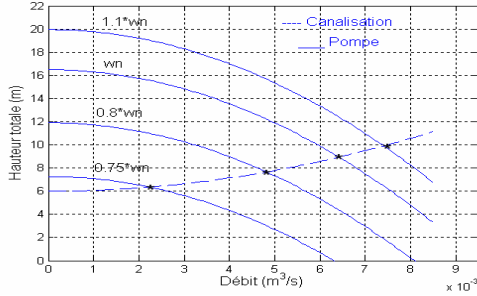


Fig 5.Characteristics H(Q).

E. Summary of Correction PI and IP

To optimize the system with given performances, the system must be controlled. The first role of a regulation system is to oblige the controlled parameters (output of the system) to preserve values as close as possible as those which one chooses like references values. Generally the control devices are with closed loop. Classically, the regulating of the stator currents is done with the PI controller. In the next section we will see the benefits brought by a regulator type IP. To test and compare these two regulators, we will submit the same operating conditions. For this command, there are three correctors used to control the speed and the two components of the stator current.[9]

F. Current Regulator PI

The proportional action is used to adjust the speed of the system dynamics and an integral action is used to eliminate the difference between the reference variable and the one you wish to enslave. The current control scheme by a PI corrector is illustrated by the following diagram: [10]

$$e_a = i_a R_a + L_a \frac{di_a}{dt} + e$$

$$e_a - e = i_a (R_a + L_a S)$$

$$i_a = \frac{1}{(R_a + L_a S)} (e_a - e)$$

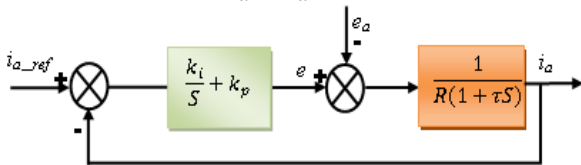


Fig.6 Block diagram of the current controller

The transfer function of the open loop system is FOL:

$$F_{OL} = K_i \left(\frac{1 + \tau S}{S} \right) \left(\frac{1}{R_a (1 + \tau S)} \right)$$

$$F_{OL} = \frac{K_i}{R_a S}$$

$$\tau = \frac{L}{R_a} = \frac{K_p}{K_i}$$

The transfer function of the closed loop system is FCL:

$$F_{CL} = \frac{F_{OL}}{1 + F_{OL}}$$

$$F_{CL} = \frac{1}{1 + \frac{R_a S}{K_i}} = \frac{1}{1 + \tau_n S}$$

$$\tau_n = \frac{R_a}{K_i}$$

$$t_r = 3\tau_n$$

$$K_i = \frac{3R}{t_r}$$

$$K_p = \frac{3L}{t_r}$$

G. Speed regulator PI

The speed controller can determine the electromagnetic torque, the mechanical equation gives:

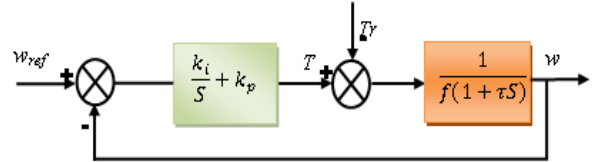


Fig.7 Block diagram of the speed controller with PI regulator
The transfer function of the open loop system is FOL:

$$F_{OL} = \left(k_p + \frac{k_i}{S} \right) \left(\frac{1}{J S + f} \right)$$

$$F_{OL} = K_i \left(\frac{1 + \tau_m S}{S} \right) \left(\frac{1}{f(1 + \tau_m S)} \right)$$

$$F_{OL} = \frac{K_i}{f S}$$

$$\tau_m = \frac{J}{f} = \frac{K_p}{K_i}$$

The transfer function of the closed loop system is FCL:

$$F_{CL} = \frac{F_{OL}}{1 + F_{OL}}$$

$$F_{CL} = \frac{1}{1 + \frac{f}{K_i S}}$$

$$\tau_N = \frac{f}{K_i}$$

$$t_r = 3\tau_N$$

$$K_i = \frac{3f}{t_r}$$

$$K_p = \frac{3J}{t_r}$$

H. Current regulator IP

A PI control on a first-order process shows a zero. This zero accelerates system response, which usually results in a transient oscillating. The corrector proportional Integral IP is essentially different from the PI corrector by the fact that there is no zero in the transfer function of the closed loop, and its output does not represent discontinuity in the application of a reference type echelon. The block diagram of the current control corrector IP is illustrated by the following figure:

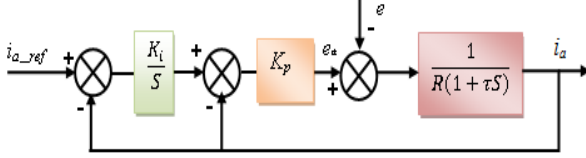


Fig.8 Block diagram of the current controller with PI regulator

In the absence of the e.m.f ($e=0$), the transfer $F_{OL}(s)$ function of the closed loop system is given by:

$$F_{OL}(s) = \frac{K_p}{R(1 + \tau s)}$$

The transfer $T(s)$ function of the final closed loop system is given by:

$$F_{CL}(s) = \frac{F_{OL}(s)}{1 + F_{OL}(s)}$$

$$F_{CL}(s) = \frac{\frac{K_i K_p}{\tau R}}{S^2 + \left(\frac{R + K_p}{\tau R}\right)S + \frac{K_p K_i}{\tau R}}$$

$$w_n^2 = \frac{K_i K_p}{\tau R} \quad 2\xi w_n = \frac{R + K_p}{\tau R}$$

$$K_p = 2\xi w_n L - R$$

$$K_i = \frac{L w_n^2}{2\xi w_n L - R}$$

I. Speed regulator IP

The block diagram of the speed control corrector IP is illustrated by the following figure: [9][11]

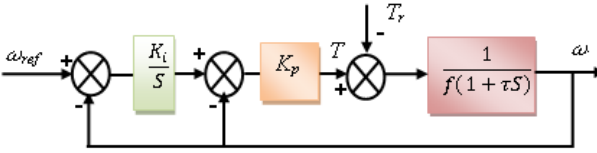


Fig.9 Block diagram of the speed controller with IP regulator

In the absence of disturbances ($C_r=0$), the transfer function of the closed loop system is given by:

$$F_{OL}(s) = \frac{K_p}{f(1 + \tau s)}$$

The transfer $T(s)$ function of the final closed loop system is given by:

$$F_{CL}(s) = \frac{F_{OL}(s)}{1 + F_{OL}(s)}$$

$$F_{CL}(s) = \frac{\frac{K_i K_p}{\tau f}}{S^2 + \left(\frac{R + K_p}{\tau m f}\right)S + \frac{K_p K_i}{\tau m f}} = \frac{w_n^2}{S^2 + 2\xi w_n S + w_n^2}$$

$$w_n^2 = \frac{K_i K_p}{\tau f} \quad 2\xi w_n = \frac{f + K_p}{\tau f}$$

$$K_p = 2\xi w_n J - f$$

$$K_i = \frac{J w_n^2}{2\xi w_n J - f}$$

III. SIMULATION RESULTS AND DISCUSSION

In this section the simulation results of the global efficiency optimization of a photovoltaic pumping system driven by DC motor coupled to a centrifugal pump are presented. The validation of this command is done using Matlab-Simulink software. The simulation results show that the two current regulators IP and IP based arrive ultimately regulate currents and speed in the machine, and that the choice of the IP controller has more satisfactory than the PI performance by either servo or regulation, both transient minimizing overshoot observed on speed and current, permanent regime (minimizing ripples), figure 14,15 thing that will automatically change the electromagnetic torque and thereafter on speed, figure 13

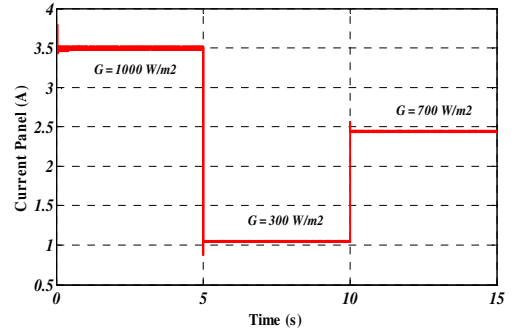


Fig.10 Current panel (A)

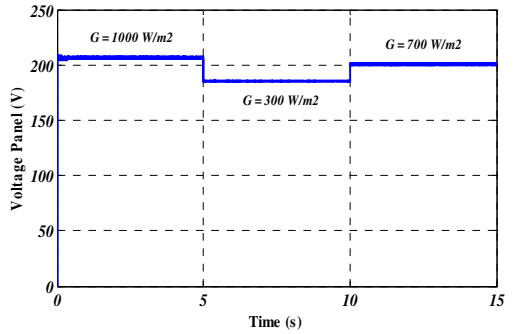


Fig. 11 Voltage panel (V)

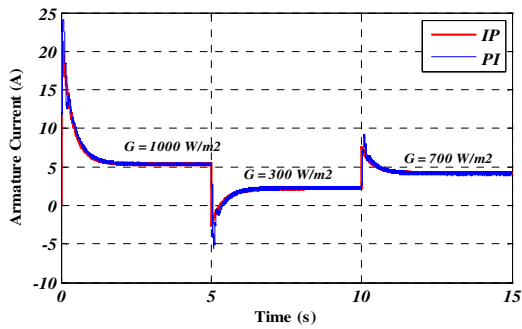


Fig.12 Armature current (A)

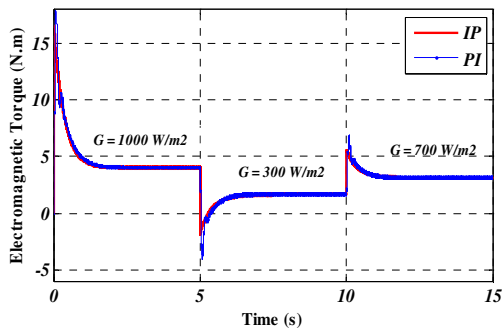


Fig.13 Electromagnetic torque (N.m)

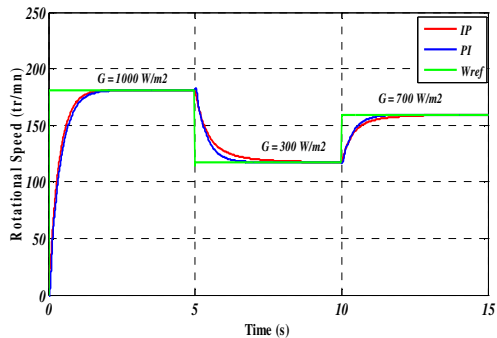


Fig.14 Rotational speed (tr/mn)

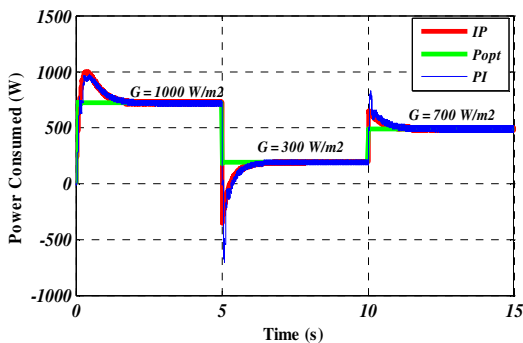


Fig.15 Power Consumed (W)

IV. CONCLUSION

In this article, we presented a comparison of performances of two controllers PI and IP of a DC machine powered by a photovoltaic generator. The robustness with respect to IP correction term in PI control for speed and current was justified theoretically and by simulation. The calculation of reference parameters and expressions of current prescription and speed, involve the parameters of the machine. The next step would be to develop control algorithms based on fuzzy logic and neural networks for updating in real time of these parameters in the control and implement these techniques on a DSP board.

REFERENCE

- [1] A.A. Ghoneim "Design optimization of photovoltaic powered water pumping systems" Applied Sciences Department, College of Technological Studies, Shuwaikh 70654, Kuwait, Energy Conversion and Management 47 (2006) 1449–1463
- [2] HUA, C.LIN, J.SHEN, C. : Implementation of a DSP Controlled Photovoltaic System with Peak Power Tracking, IEEE Trans. Ind. Electronics 45 No. 1 (Feb 1998), 99{107.
- [3] Blaschke F, 1972. *The principle of field orientation as applied to the new transvector closed-loop control system for rotating-field machines*. Siemens Rev.
- [4] Townsend TU. A method for estimating the long-term performance of direct-coupled photovoltaic system. MSc thesis. Mechanical Engineering, University of Wisconsin—Madison, 1989.
- [5] Ghoneim AA, Al-Hasan AY, Abdullah AH. Economic analysis of photovoltaic powered solar domestic hot water systems at Kuwait. *Renew Energy* 2002;25:81–100.
- [6] Bloss H, Gabler H, Janssen A, Moraes R. Analytical and experimental investigation of the performance of PV-pumping systems. In: *ISES Conference, Zimbabwe, 1995*.
- [7] Benlarbi, K. et al., 2004."A fuzzy global efficiency optimization of a photovoltaic water pumping system". *Solar Energy* 77, 203–216.
- [8] Kamal Himour, Kaci Ghedamsi" Performance Optimization of a Photovoltaic Water Pumping System" Copyright IPCO-2014 Vol.2.
- [9] Jebali T., Jemli M., Boussak M., Gossa M. et Kamoun M.B.T, 2004. Dspace-based experimental results of indirect field oriented control (IFOC) PWM VSI fed induction motor. In proceedings IEEE-ICIT'04, *International Conference on Industrial Technology*, vol. 2, p. 569-573. Hammamet, Tunisia.
- [10] Baghli L., Razik H. et Rezzoug A ,1996. A field oriented control method usingdecoupling terms for induction motors. In *Proc. 2nd EPE Chapter symposium on electric drive design and applications*, p.147-151, Nancy, France.
- [11] Jarray, K., 2000 Contribution à la commande vectorielle à flux statorique orienté d'un actionneur asynchrone avec et sans capteur mécanique. Thèse de doctorat de l'université de droit, d'économie et des sciences d'AIX MARSEILLE.